



# Assessment of groundwater salinity using GIS and multivariate statistics in a coastal Mediterranean aquifer

H. Ferchichi<sup>1</sup> · M. F. Ben Hamouda<sup>2</sup> · B. Farhat<sup>1</sup> · A. Ben Mammou<sup>1</sup>

Received: 20 August 2017 / Revised: 5 February 2018 / Accepted: 11 May 2018 / Published online: 7 June 2018  
© Islamic Azad University (IAU) 2018

## Abstract

The integration of the statistical approaches and GIS tools with the hydrogeological and geological contexts allowed the assessment of the processes that cause groundwater quality deterioration in the great important deltaic aquifer in the north-eastern Tunisia (Medjerda Lower Valley Aquifer). The spatial variation of the groundwater parameters and the molar ratio ( $\text{Cl}^-/\text{Br}^-$ ) were also used to determine the possible impacts from seawater intrusion and from the septic tank leachate. Sixty shallow groundwater samples were collected in 2014 and analyzed for major and trace ions over an area of about 1090 km<sup>2</sup> to determine the suitability for drinking or agricultural purposes. The total dissolved solids (TDS) content ranges from 1005 to 19,254 mg l<sup>-1</sup> with a mean value of 3477.18 mg l<sup>-1</sup>. The chemistry is dominated by the sodium–chloride waters (55%). Mapping of TDS,  $\text{Cl}^-$ ,  $\text{Na}^+$ ,  $\text{SO}_4^{2-}$  and  $\text{NO}_3^-$  using kriging method shows a clear increase in salinity toward the coastline accompanied by  $\text{Na}^+$  and  $\text{Cl}^-$  increase which may be related to seawater intrusion and halite dissolution. Locally, higher nitrate concentration is related to the agricultural activities inducing contribution of chemical fertilizers and irrigation with treated wastewater. The saturation indices indicate that all carbonate minerals tend to reach saturation equilibrium confirming water–rock interactions, while evaporitic minerals are still in sub-saturation state and may increase the salinity of the groundwater. The principal component analysis proves the occurrence of groundwater contamination principally by seawater intrusion in the factor I (74.15%) and secondary by an anthropogenic source in the factor II (10.35%).

**Keywords** Groundwater salinization · Hydrochemistry · Geostatistics · Coastal aquifer · Tunisia

## Introduction

Groundwater is the most important natural resource which influences sustainable socioeconomic development of every community. Water resources are harnessed for different purposes such as agricultural, domestic and industrial activities; therefore, it is important to protect this resource from contamination (Loucks and Jia 2012). In these recent decades, the contamination of groundwater is rated as of the most serious problems worldwide, especially in arid and semiarid

areas. Salinization processes are very complex and may be due to many factors such as climate, topographic relief, geology, saline water intrusion, recycling of wastewaters, drainage system, irrigation return flows and septic tank leachate (e.g., Holly et al. 2005; De Montety et al. 2008; Samsudin et al. 2008; Park et al. 2005; Selvam et al. 2014; Kaliraj et al. 2014; Jia et al. 2015; Bodrud-Dozaa et al. 2016; Tringali et al. 2017). Understanding factors that control the quality degradation of groundwater, which are more sensitive over years, due to the intensive use of the natural resources and increased human activities, is an academic challenge and has a significant practical implication for water resource management (Bouchaou et al. 2008).

A great number of papers involve multivariate statistics to identify the possible factors that influence groundwater salinization processes and offer a robust tool for water resources management as well as quick solution to pollution problems in many parts of the world in both coastal and non-coastal areas (Fakir et al. 2001; Zghibi et al. 2014; Chenini et al. 2015; Molla et al. 2015; Bodrud-Dozaa et al.

Editorial responsibility: U.W. Tang.

✉ H. Ferchichi  
hajer2682@yahoo.fr

<sup>1</sup> Faculty of Sciences of Tunis, Department of Geology, Mineral Resources and Environment Laboratory (LRME), University of Tunis El Manar, 2092 Tunis, Tunisia

<sup>2</sup> UMTN, Isotope Hydrology and Geochemistry Unit, CNSTN, Technopark of Sidi Thabet, 2020 Sidi Thabet, Tunisia



2016). In this first multidisciplinary study, two multivariate statistical analyses of groundwater quality data were applied: the hierarchical cluster analysis (HCA) and the principal component analysis (PCA) to deduct the zones of potential contamination. The data obtained from the laboratory analysis were used as variable inputs for factor analysis which is an important useful statistical tool for the geochemical data interpretation to evaluate the factors governing the behavior of the aquifer system (Davis 1986; Papatheodorou et al. 2007; Zghibi et al. 2014).

During the last decades, the north of Tunisia displays rapid social and economical development making growing needs for industrial, agricultural and drinking water supply. In the MLV area, the groundwater appears the main source of freshwater. However, this vital resource is increasingly deteriorated and the processes that affect groundwater chemistry are not well understood. Face to this critical situation, the assessment of the groundwater quality needs more attention and its management becomes a necessity.

Several studies have provided preliminary indications on the salinization of the groundwater of the shallow MLV aquifer (Ammar 1989; El Guarouani et al. 1999; Samaali 2011; Ben Ammar et al. 2014, 2016; Andolsi 2016). The aim of this work is to explore and identify the different processes that affect groundwater quality in the MLVA through a survey sampling made in September 2014. Therefore, several assessing methods were carried out by the mean of geographic information systems “GIS” tools and geochemical and statistical analysis. Moreover, mapping of chemical parameters using GIS is used to determine the groundwater contamination extent maps by overlaying the available data (topography, geology, hydrology, hydrogeology, geochemistry, etc.). Ordinary kriging interpolation method is used for showing initial decision of spatial distribution of groundwater parameters. Such understanding will contribute to upgrade land management and improve water planning strategies.

## Materials and methods

The MLVA covers an area extent of about 1090 km<sup>2</sup> (Fig. 1). The hilly landscape of the region is part of the large coastal plain and slopes to the north and north–northwest with elevations decreasing from 418 m (Jb. Kechabta) and 325 m (Jb. Ennadhur) to 0 m above sea level. It is bordered to the west by the crest line of several mountains: Jb. Sakkak, Jb. Oued el Melah and Jb. Lansarine which reach a maximum altitude of 565 m. To the south, it is bounded by the crest line of Jb. Naheli (236 m) and Jb. Ammar (323 m). The Mediterranean Sea forms the eastern limit. Following the topography, two different climate environments are found: a coastal environment with marine influence and a semi-continental mountain

environment. The climate is defined by a Mediterranean bioclimatic top floor semiarid, with mild and wet winters and dry and hot summers. The rainfall is characterized by a high irregularity with an average annual precipitation of about 450 mm per year (INM 2015). The mean annual temperature is 20 °C, with a minimum of 8 °C and a maximum of 45 °C (INM 2015). The potential evapotranspiration (ETP) is very high  $\approx$  1300 mm/year.

Climatic and topographic conditions are very favorable for expanded agriculture near the Medjerda River and Ghar El Melh Lake. The study area belongs to the Atlas zone of Tunisia. Six topographic maps and six geological maps of scale 1:50,000 covering the study area and including the location of groundwater samples were scanned. Recently, Boutib (1998), Kacem (2004), Samaali (2011) and Mejri (2012) described the regional geology of the north of Tunisia. Geophysical investigations (Melki 1997; Ouerghi 2014), seismic profiles and boreholes allowed more details to understand the hydrogeology of the MLVA. In outcrop, the lithostratigraphy ranges from the Triassic evaporitic series, Jurassic carbonates, Cretaceous series until the sedimentary Mio-Plio-Quaternary series (Fig. 2a). These stratigraphic series are the field of cutting blocks with a set of major faults in many directions; the most frequent are the northwest–southeast, northeast–southwest and north–south. The Triassic is always in an abnormal position in tectonic contacts. This can be seen outcropping in Jb. Ammar which corresponds to an anticline structure-oriented northeast–southwest which core is pierced by a large injected Triassic fault (Fig. 2b) (Pini et al. 1971). The available carbonates and sulfates in these rocks might have been dissolved and added to the groundwater system during rainfall infiltration, irrigation and groundwater movement. The Quaternary sediments occupy almost 60% of the study area. The Medjerda delta is largely covered with Quaternary sediments with an elevation ranging from 5 to 8 m above sea level to the west, 0 to 2 m near the shoreline. These Quaternary outcrops are represented by two predominant levels: the first silty level is often encrusted on which muddy silt occupies lake and lagoon; the second silty level is an interbedded conglomeratic forming the basis of the series (Pini et al. 1971; Bahri 1993).

The deltaic basin benefits both from the runoff of the watershed and from the underground flow of the geological structures surrounded, which have given to the reservoir a vast synclinal basin (Ammar 1989). The drainage network consists essentially by the greater perennial river in Tunisia (Medjerda River which collect the surface runoff from the mountainous areas) and secondary tributaries of which the outflow is toward the Mediterranean Sea. The shallow aquifer is lodged in the colluvial series of the mountains and the alluvial fillings of the plain. It is characterized by a relatively low renewal rate. From lithology and structural configuration, carbonate sediments (Jurassic and Cretaceous)



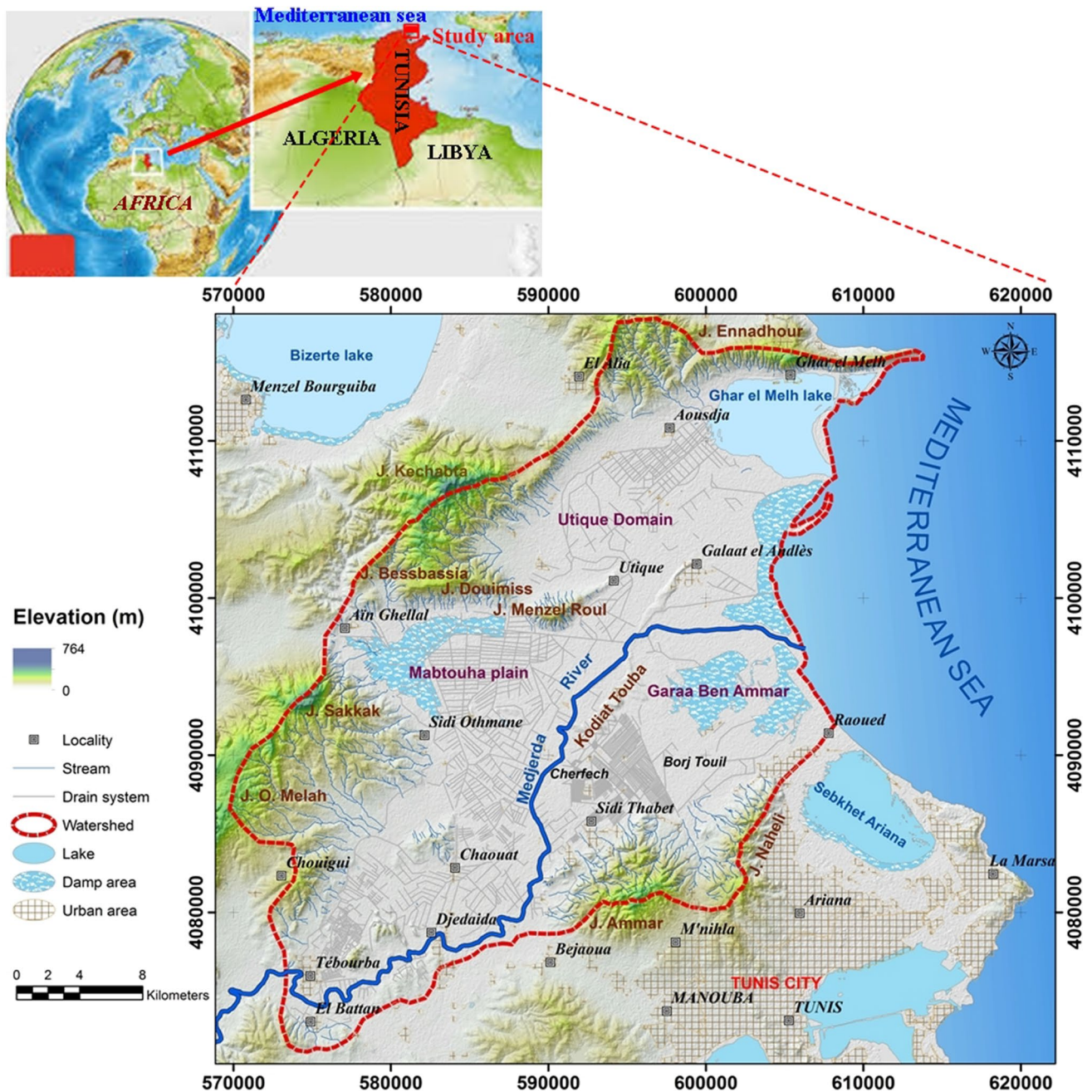


Fig. 1 Location map showing topographic and hydrographic framework of the study area (SRTM resolution of 30 m)

and sandstones (Mio-Pliocene) of hills bordering the Utique Domain and the Mabtouha plain (potential aquifer) may contribute to the supply of the aquifer in the upstream part. In the southern part, the underground supplies are assured by the flows from Jb. Ammar and Jb. Naheli.

The sampling of groundwater within the study area was carried out during September–October 2014 from the MLV area. In the present study, all the samples were collected in equilibrium state of the aquifer, which can well represent the groundwater quality. A total of 60 samples were collected

for private and public wells from the shallow aquifer. Water samples from freshwater (Medjerda River) and marine water were also collected. Sampling has not been able along the coastal zone because the water table rising to the surface (Static level  $\leq 5$  m) and wells do not exist because the salinity of the groundwater is too high and this coastal area is dominated by the swamps. On the other hand, toward the western mountain areas, sampling cannot be able (because it is inaccessible) and the slope sides display the hydrogeological limit of the shallow LVMA. For this, sampling beyond



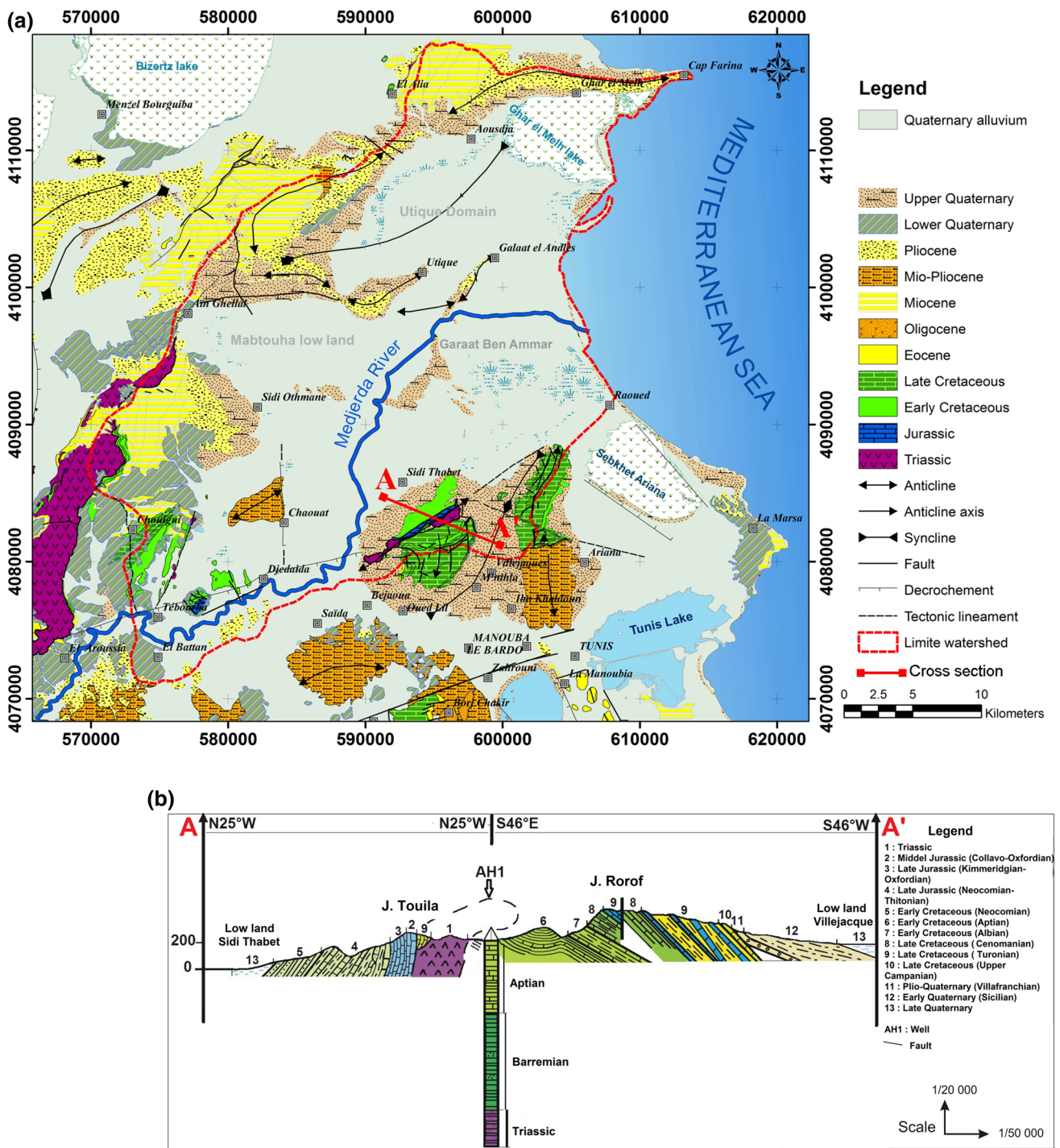


Fig. 2 a Simplified geological map of the study area with main tectonic faults and b geological cross section (AA') from Triassic to Quaternary in Jebel Ammar modified after Pini et al. (1971)

the study area will distort the results. The location of the groundwater samples is shown in Fig. 4. The selected wells are uniformly distributed over the area of concern. The sampling bottles soaked in 1:1 HCl for 24 h and were rinsed with distilled water followed by deionized water. In the field, the sampling bottles were thoroughly rinsed two or three times,

using the groundwater to be sampled after pumping for 10 min. This was done to remove groundwater stored in the well. Field measurements including temperature (T), electrical conductivity (EC) and pH were taken using a multi-parameter WTW (Thermo Russel Model pH meter) and a pH-T-EC meter. Water samples were collected in 1000-ml



polyethylene bottles with poly-seal caps for major and trace elements. The groundwater sampled bottles were labeled, tightly packed, transported immediately to the laboratory. Samples destined for laboratory analyses were immediately filtered through 0.45- $\mu\text{m}$  filters on acetate cellulose and collected in acid-rinsed 100-ml polyethylene bottles and stored at 4 °C for chemical analyses. Chemical analyses of the water samples were undertaken, using standard methods, at Isotope Hydrology and Geochemistry Laboratory, National Center for Nuclear Sciences and Technologies (CNSTN), Technological pole of Tunisia.

Major and minor elements (such as chloride ( $\text{Cl}^-$ ), sulfate ( $\text{SO}_4^{2-}$ ), nitrate ( $\text{NO}_3^-$ ) and bromide ( $\text{Br}^-$ )) were analyzed by the means of high-performance ion chromatography produced by DIONEX Co. Magnesium ( $\text{Mg}^{2+}$ ) and calcium ( $\text{Ca}^{2+}$ ) concentrations were determined in the laboratory by the titration method using 0.02 N ethylenediaminetetraacetic (EDTA) acid. The alkalinity (bicarbonate ( $\text{HCO}_3^-$ ) concentration) was also determined by the titration using 0.1 N HCl acid. The concentrations of sodium ( $\text{Na}^+$ ) and potassium ( $\text{K}^+$ ) were measured by the atomic emission spectrophotometry method.

The charge balance definition and the chemical analyses for charge balance were defined according to the Freeze and Cherry (1979) as follows:

$$\% \text{ Charge balance error} = \left( \sum z \times m_c - \sum z \times m_a \right) / \left( \sum z \times m_c + \sum z \times m_a \right) \times 100$$

where  $z$  is the absolute value of the ionic valence,  $m_c$  is the molality of cationic species and  $m_a$  is the molality of the anionic species. The value of the charge balance error for the chemical analyses may be within the acceptable limit of  $\pm 5\%$  of all the hydrochemical dataset. The suitability of groundwater for domestic or agricultural purposes was estimated by comparing the values of the groundwater quality constituents with those of the World Health Organization (WHO 2004).

Hydrochemistry of the MLV shallow aquifer was summarized via the statistical analysis of groundwater properties. Hierarchical cluster analysis (HCA) and principal component analysis (PCA) were applied to evaluate their usefulness to classify the groundwater samples and to identify geochemical processes controlling groundwater geochemistry. All the statistical calculations were performed using Statistica 8 software. PCA has been used frequently in geochemical studies (Ruiz et al. 1990; Morell et al. 1996; Papatheodorou et al. 2007; Charfi et al. 2013; Sekiou and Kellil 2014; Zghibi et al. 2014; Masoud 2014; Machiwal and Jha 2015; Molla et al. 2015; Bodrud-Dozaa et al. 2016). Factor analysis is used to transform the initial data into a new set of composite variables or principal components which will be

classified according to their variances (BRGM 2001). This method has been frequently used to grouping the commonly collected water quality data, where each cluster indicates the water of a particular quality. The GIS platform (using ARCGIS 10.1 software) allows the generation of the spatial distribution of several parameters in this study. Spatial pattern of groundwater quality parameters, over the area, such as TDS, sodium, chloride, nitrate and sulfate concentrations, was carried out using kriging method. Kriging is the most important geostatistical technique that generates an estimated surface from scattered points with  $z$ -values. Using kriging tool implies an interactive investigation of the spatial behavior of the phenomenon represented by the  $z$ -values before selecting the best estimation method for generating the output surface (ESRI, 2017).

Bromide is considered as a trace element in the earth's crust. In seawater, bromide has a concentration of 66–68 mg/l, which is about 300 times lower than the typical concentration of chloride. Both ions move conservatively in water, and they have different abundances in natural solids and fluids (Davis et al. 1998). In this study,  $\text{Cl}^-/\text{Br}^-$  mass ratio was used for assessing possible origins of shallow groundwater contamination from wastewater sources (such as septic tank leachate) or other anthropogenic or natural (such as seawater intrusion). The adapted methodology in this study is summarized in the flowchart as follows (Fig. 3).

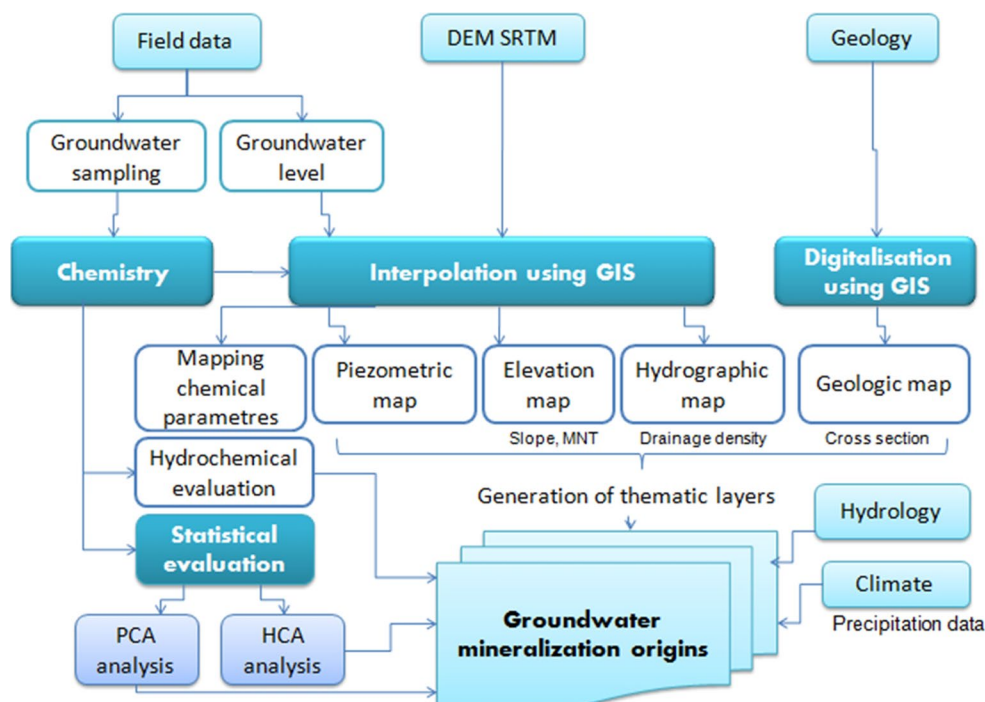
## Results and discussion

The results obtained from the chemical analyses and field measurements for the ground and surface water samples in LVM are summarized in Table 1. All chemical parameters reveal very wide ranges and important standard deviations. Specially, electrical conductivity (EC) which is ranging from 1.4 to 29.2 mS/cm (EC seawater = 66.8 mS/cm) and pH values ranging from 6.9 to 8.8 (mean 7.3) indicate slightly acidic to slightly alkaline waters (Table 2). The TDS variation is within 1005 and 19,254 mg/l with a mean value of about 3477.18 mg/l. These values are above the maximum permissible limit (1000 mg/l) of the WHO's drinking water guideline (WHO 2004). All of them are classified as brackish ( $1000 \text{ mg/l} \leq \text{TDS} \leq 10,000 \text{ mg/l}$ ) except the samples 26, 27 and 29 which are saline.

The dominance of anions was classified in the order of  $\text{Cl}^- > \text{SO}_4^{2-} > \text{HCO}_3^- > \text{NO}_3^-$  with the means values, respectively, of 1026.67; 773.196; 446.133 and 73.52 mg/l, while the dominance of cations was  $\text{Na}^+ > \text{Ca}^{2+} > \text{Mg}^{2+} > \text{K}^+$  with the means values, respectively, of 710.31; 267.939; 126.716; and 42.358 mg/l. The ions  $\text{Na}^+$  and  $\text{Cl}^-$  present high variations between minimum and maximum values (similar coefficient of variation, respectively, 94.141 and 94.485). The  $\text{Na}^+$  concentration increase is accompanied by a parallel



**Fig. 3** Flowchart showing the adopted methodology



$\text{Cl}^-$  concentration increase, whence a sodium–chloride facies dominant. Likewise,  $\text{SO}_4^{2-}$  and  $\text{NO}_3^-$  are highly variable with standard deviations larger than the mean. Such wide ranges recommend that the chemistry of the MLVA is not homogenous.

Fluoride represents one of the main trace elements in groundwater, which generally occurs as a natural constituent. The concentration of fluoride in groundwater of the MLVA varied between 0 and 45 mg/l. The majority of the groundwater samples have higher fluoride content than the acceptable limit for drinking water (1.5 mg/l) (WHO 2004). The elevated fluoride values are mainly attributed to the application of chemical fertilizers in the agriculture. Bromide is a minor natural ion in groundwater and can be used as an indicator of the mixture with an heterogeneous source of water. Bromide concentrations in the samples from MLVA ranged from 0 to 39 mg/l. The coastal groundwater samples have slightly higher bromide concentrations mainly due to the seaborne aerosols and the seawater intrusion.

### Groundwater types

The chemical composition of the groundwater samples was plotted on the Piper trilinear equivalence diagrams using Diagramme software shown in Fig. 4a. The groundwater reflects main different hydrochemical facies. The data plots in the Piper diagram show that  $\text{Na}^+$  and  $\text{Ca}^{2+}$  of cation and  $\text{Cl}^-$  and  $\text{SO}_4^{2-}$  of anion parameters are predominant. The plot reveals that the main water type is  $\text{Na}^+-\text{Cl}^-$  (55%). According to Pulido-Leboeuf 2004, when

groundwaters show  $\text{Na}^+-\text{Cl}^-$  type dominant, they generally indicate a strong seawater influence. The other groundwater types less dominant are:  $\text{Na}^+ > \text{Ca}^{2+}-\text{Cl}^- > \text{SO}_4^{2-}$  mixed (15%),  $\text{Na}^+ > \text{Ca}^{2+}-\text{Cl}^-$  (10%),  $\text{Na}^+-\text{Cl}^- > \text{SO}_4^{2-}$  (6.7%),  $\text{Na}^+-\text{Cl}^- > \text{HCO}_3^-$  (5%),  $\text{Na}^+ > \text{Ca}^{2+} > \text{Mg}^{2+}-\text{Cl}^- > \text{SO}_4^{2-}$  mixed (3.3%),  $\text{Ca}^{2+}-\text{Cl}^- > \text{SO}_4^{2-}$  (3.3%) and  $\text{Na}^+ > \text{Mg}^{2+}-\text{Cl}^- > \text{HCO}_3^-$  mixed (1.7%) types. The groundwater types indicate that the groundwater chemistry is controlled by cations exchange reactions, as well as simple mixing (Richter and Kreitler 1991; Appelo and Postma 2005; Lee and Song 2007).

### Water suitability for irrigation use

As regards groundwater irrigation suitability, water mainly depends on the concentration of total soluble salts which can be adequately defined in terms of electrical conductivity. Sodium adsorption ratio (SAR) is the main criterion to determine the quality of irrigation water. This parameter denotes the relationship between sodium concentration in the irrigation water, magnesium and calcium. Calcium and magnesium must tend to counter the negative effect of sodium. SAR has become necessary for the reason that surface water was not always available and irrigation has wholly relied on groundwater. The groundwater with high SAR level is not suitable for agricultural purpose, which can apply a long-term soil changes and damage as it tends to breakdown of soil structure (become hard and compact) and water infiltration problems causing problems with crop production. Sandy soils are not affected by the sodium (because of the low clay content), but the plants growing on them may be affected.

**Table 1** Chemical data of the MLV groundwater samples

Num	Group	P.L (m)	pH	E.C (mS cm <sup>-1</sup> )	RS (mg/l)	TDS (mg/l)	Ca <sup>2+</sup> (mg/l)	Mg <sup>2+</sup> (mg/l)	Na <sup>+</sup>	K <sup>+</sup>	(mg/l)					Charge bal- ance error %	
											SO <sub>4</sub> <sup>2-</sup>	Cl <sup>-</sup>	NO <sub>3</sub> <sup>-</sup>	HCO <sub>3</sub> <sup>-</sup>	F <sup>-</sup>		Br <sup>-</sup>
3	Surface water	7.9	7.9	3.8	3750	2620	213	78	591	11	626	723	11	366	5	3	4
2	Group 1: TDS < 2000 mg/l	11.4	8.2	2.3	1530	1881	120	80	363	52	236	477	6	546	3	1	5
8		10.6	7.1	2.2	2230	1658	192	56	230	4	270	424	35	446	5	6	-2
11		10.1	7.0	2.7	1729	1984	228	63	260	95	408	396	57	477	1	1	4
13		2.9	7.1	2.7	1742	1984	205	116	258	5	446	443	12	496	3	3	2
28		3.8	7.9	2.0	1275	1351	116	43	267	9	266	360	37	254	6	1	2
31		43.0	7.2	3.3	2158	1902	189	101	237	10	555	553	48	210	4	0	-5
40		15.5	7.1	3.7	2226	1168	50	78	143	7	147	255	149	339	3	2	-5
42		20.7	7.4	3.6	2142	1090	76	53	189	2	194	269	92	215	2	3	0
43		13.7	7.1	1.4	930	1483	136	73	230	4	195	355	122	368	2	13	2
46		11.6	7.3	3.8	2269	1633	68	35	350	42	341	344	100	353	5	3	-3
47		7.5	7.5	2.3	1482	1005	44	27	219	9	90	310	7	299	1	1	-4
49		8.6	7.4	3.3	2165	1383	52	69	274	10	195	473	14	298	1	4	-4
50		3.8	7.2	2.1	1378	1483	68	74	232	73	157	423	5	450	1	1	-2
52		4.7	7.6	2.5	1645	1660	152	80	205	6	421	355	69	373	0	3	-5
54		3.9	7.7	2.6	1881	1842	137	71	294	90	303	699	15	232	4	1	-4
55		9.5	6.9	2.3	1657	1782	135	94	269	14	441	564	41	224	3	1	-5
4	Group 2: 2000 < TDS < 4000 mg/l	11.9	7.0	5.0	4980	3526	316	84	771	33	648	956	104	614	5	4	5
5		11.9	7.0	4.1	4050	2631	290	84	481	16	556	677	63	465	2	3	5
6		10.9	7.2	3.6	3630	2604	176	143	497	13	535	714	5	521	2	4	4
7		12.4	7.3	3.0	2950	2116	296	94	212	7	561	464	60	422	3	2	-1
9		10.9	7.0	2.9	2930	2200	196	113	292	2	440	513	155	490	0	3	-3
10		14.5	7.1	4.5	2670	3069	352	169	481	8	663	907	43	446	3	4	5
12		6.8	7.7	3.0	1918	2411	160	116	444	21	538	731	5	397	3	2	5
14		5.6	6.9	3.4	2204	2313	276	81	338	29	477	485	88	539	3	3	3
15		2.4	7.0	2.9	1898	2051	178	109	338	31	423	470	61	440	3	4	5
16		-5.3	7.3	4.2	2502	3322	348	213	439	51	743	885	16	626	3	3	5
19		6.0	7.1	4.4	2628	3385	320	143	605	6	745	977	137	453	3	8	2
21		6.7	7.5	4.0	2418	2876	292	92	557	12	445	916	147	415	3	8	3
22		5.2	7.6	3.3	1974	2587	250	99	465	12	568	709	69	415	3	3	2



Table 1 (continued)

Num	Group	P.L (m)	pH	E.C (mS cm <sup>-1</sup> )	RS (mg/l)	TDS (mg/l)	Ca <sup>2+</sup> (mg/l)	Mg <sup>2+</sup> (mg/l)	Na <sup>+</sup>	K <sup>+</sup>	(mg/l)				Br <sup>-</sup> %	Charge bal- ance error %	
											SO <sub>4</sub> <sup>2-</sup>	Cl <sup>-</sup>	NO <sub>3</sub> <sup>-</sup>	HCO <sub>3</sub> <sup>-</sup>			F <sup>-</sup>
23		5.6	7.4	7.0	4224	3268	544	174	274	7	1265	485	17	502	1	1	5
30		30.7	7.0	3.1	2039	2251	151	77	513	14	587	617	35	256	4	0	3
32		23.0	7.0	3.7	2435	2179	218	105	338	8	578	583	81	267	4	0	1
34		9.8	7.2	5.5	3300	3121	240	94	715	25	541	910	5	590	5	4	5
35		8.8	7.1	2.7	1768	2159	88	57	462	42	202	405	233	670	7	3	4
38		2.3	7.5	4.1	2460	3353	276	50	741	4	532	881	63	806	4	8	0
39		0.7	7.6	3.5	2094	2410	99	55	635	13	411	756	32	409	4	1	1
41		14.7	7.5	1.6	1066	2387	236	56	393	27	457	549	227	441	5	9	-2
44		47.5	7.2	2.8	1820	2529	184	34	598	4	549	735	65	360	4	9	-1
45		10.0	7.3	5.1	3110	3344	88	160	872	14	830	893	5	482	4	4	5
48		13.0	7.4	1.8	1144	2390	56	128	501	73	308	773	43	506	8	2	0
51		7.6	7.3	2.3	1460	2592	304	126	288	12	625	635	75	527	1	4	-3
56		9.5	7.6	3.6	2765	2988	194	90	690	6	765	877	16	350	5	1	1
58		20.1	7.2	6.2	4066	3999	251	123	895	28	488	1674	67	474	6	1	-3
59		25.4	7.2	5.0	3452	3112	179	87	754	21	674	944	65	388	5	1	2
1	Group 3: TDS > 4000 mg/l	11.1	7.0	6.6	3985	5028	346	183	1141	19	1337	1329	72	1	7	6	4
17		7.8	7.2	4.6	2760	4072	250	117	957	11	716	1314	69	639	5	6	1
18		3.9	8.8	7.0	4218	5975	249	222	1610	48	1441	1958	5	440	7	8	5
20		5.8	7.0	7.1	4254	5377	553	295	879	55	1525	1548	70	453	7	8	5
24		9.4	7.2	7.0	4176	5674	541	212	1051	36	1457	1637	237	502	8	6	2
25		9.3	7.3	9.5	5682	7842	690	233	1762	3	1658	2486	596	415	9	8	4
26		2.9	7.5	29.2	17,520	19,254	1610	826	3698	796	5757	5968	17	583	45	39	5
27		1.4	7.1	14.1	8460	11,191	542	173	2912	229	2895	3750	9	682	11	9	-1
29		4.8	7.1	15.4	9240	11,043	810	445	2387	224	2984	3572	5	614	9	8	4
33		32.5	7.1	8.7	5622	6626	448	211	1553	7	1753	1988	210	457	8	6	2
36		6.9	7.5	6.7	4020	4457	220	64	1217	67	514	1624	92	660	6	6	2
37		6.2	7.0	6.8	4080	4468	276	129	1143	8	666	1485	17	744	5	3	5
53		14.3	7.0	5.0	2990	4576	244	84	1348	10	508	1885	55	441	7	6	4
57		15.7	7.5	5.6	4019	4489	288	136	1056	2	961	1486	85	474	5	2	1
60	Seawater	0.0	8.5	66.8	4476	39,440	1740	2412	10,695	421	5371	22,663	1	970	66	66	0

P.L piezometric level; EC electrical conductivity

So, the following discussion relates mostly to clays. Therefore, as regards groundwater irrigation suitability, United States Salinity Laboratory Staff (USSL 1954) helps to interpret the combined effect of salinity and sodium hazards. The SAR may be determined by the following formula:

$$\text{SAR} = \text{Na} / [\text{Ca} + \text{Mg} / 2]^{0.5}$$

Sodium, calcium and magnesium are in meq/l.

In this case study, according to the USSL diagram (Fig. 4b), most of the groundwater samples for agricultural purposes fall under C4S2 with high salinity and medium alkalinity hazards; they are classified unsuitable for irrigation. Based on this classification, the rest of the samples tend from C4S3 to C5S5 classes with high and very high salinity to very high alkalinity hazards, respectively. Furthermore, a management plane to control the salinity of the groundwater becomes necessary.

### Correlation matrix

The correlation matrix allows the evaluation of the correlation coefficients “*r*” between groundwater quality parameters. These coefficients are used to quantify the intensity of linear correlation between the variables 2–2. From Table 3, mineralization is principally related to sodium and chlorides. Strong correlation can be identified between TDS, Na<sup>+</sup> and Cl<sup>-</sup>: Cl<sup>-</sup>/TDS (*r*=0.98) and Na<sup>+</sup>/TDS (*r*=0.99). It is found that the salinity load in groundwater is controlled first by Na<sup>+</sup> and then by Cl<sup>-</sup>. Na<sup>+</sup> is the most major cation

which exhibits high positive correlation with Cl<sup>-</sup> (*r*=0.94). According to De Montety et al. (2008), in coastal semiarid regions, the Na<sup>+</sup>/Cl<sup>-</sup> relationship has frequently been used to establish the mechanisms for acquiring saline intrusion. The large contents of Na<sup>+</sup> and Cl<sup>-</sup> observed in almost all samples may confirm the dissolution of chloride salts because the dissolution of halite (NaCl) in water releases equal concentrations of both sodium and chloride ions into the solution. This can be used as an indicator of water–rock interaction.

Calcium, magnesium and sulfates participate secondarily in the mineralization of groundwater Ca<sup>2+</sup>/TDS (*r*=0.91); Mg<sup>2+</sup>/TDS (*r*=0.96); and SO<sub>4</sub><sup>2-</sup>/TDS (*r*=0.91). It can be attributed to geogenic sources from the basement rocks or anthropogenic origins of salinity. This case of regional contamination from domestic waste, treated wastewater and agricultural activities (excessive use of fertilizers) explains the complexity of the processes that control the chemistry of the groundwater, especially the nitrates increase. Furthermore, the negative correlation related to the nitrates with the other parameters may be attributed to the excessive use of the agricultural fertilizers or the septic tank leachate.

### Geochemical stability

To examine which minerals can dissolve or precipitate within the aquifer, the saturation state of groundwater with respect to selected mineral phases was computed with the aid of PHREEQC program. The calculation of the saturation indices (SIs) of different minerals of the MLVA indicates

**Table 2** Summary of the used chemical data of the groundwater in the 2014 sampling campaign (mg/l), with basic statistics

Variables	Valid N	Mean	Median	Minimum	Maximum	Variance	SD	Coef. var.
TDS	59	3477.19	2592.00	1005.00	19,254.00	8,583,136.09	2929.70	84.25
Ca <sup>2+</sup>	59	267.94	220.00	44.00	1610.00	55,999.06	236.64	88.32
Mg <sup>2+</sup>	59	126.72	93.84	27.36	825.60	13,554.16	116.42	91.88
Na <sup>+</sup>	59	710.31	480.70	142.60	3698.40	447,150.78	668.69	94.14
K <sup>+</sup>	59	42.36	12.87	1.95	795.60	11,845.56	108.84	256.95
SO <sub>4</sub> <sup>2-</sup>	59	773.20	541.48	90.00	5756.88	758,959.49	871.18	112.67
Cl <sup>-</sup>	59	1026.67	723.28	255.14	5968.00	940,928.31	970.01	94.48
NO <sub>3</sub> <sup>-</sup>	59	73.53	60.25	4.83	596.00	8313.27	91.18	124.00
HCO <sub>3</sub> <sup>-</sup>	59	446.13	446.40	1.00	806.00	20,707.52	143.90	32.26
F <sup>-</sup>	59	4.92	3.84	0.23	52.63	45.83	6.77	137.50
Br <sup>-</sup>	59	4.59	3.20	0.23	38.50	27.81	5.27	115.01
SI anhydrite	59	-1.08	-1.04	-2.18	0.14	0.19	0.44	-40.55
si aragonite	59	0.35	0.34	-0.43	1.62	0.15	0.39	112.88
SI calcite	59	0.49	0.48	-0.29	1.77	0.15	0.39	80.07
SI dolomite	59	1.02	1.04	-0.40	3.84	0.55	0.74	72.68
SI gypsum	59	-0.86	-0.82	-1.96	0.36	0.19	0.44	-50.84
SI halite	59	-5.06	-5.12	-6.06	-3.47	0.32	0.57	-11.26

N number of samples except seawater sample

**Fig. 4 a** Piper diagram for the groundwater samples labeled according to their groundwater clusters and **b** a plot of SAR against EC (USSL 1954). Water samples are according to their clusters

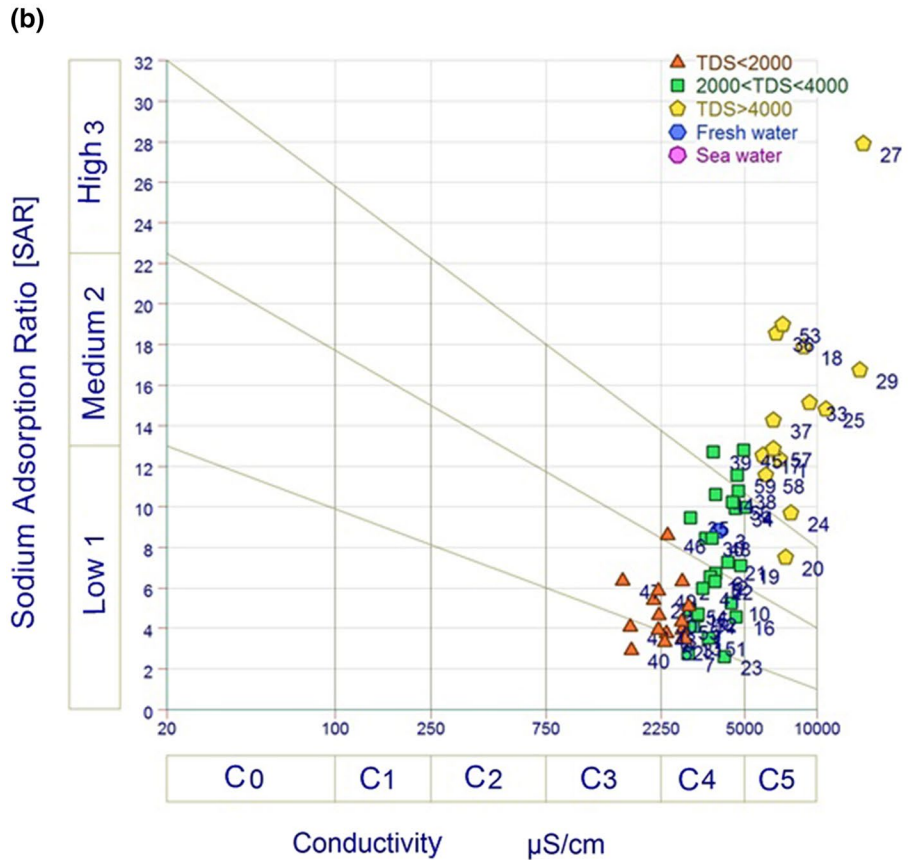
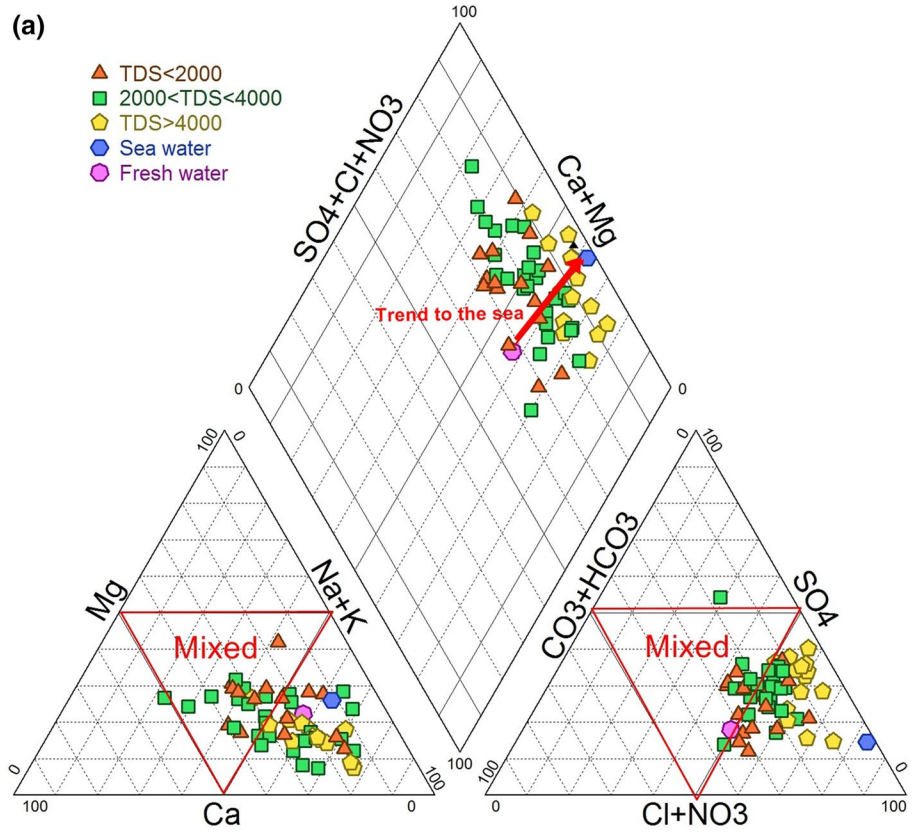




**Table 3** Correlation matrix between variables of the LVMA samples, 2014

Variables	E.C	TDS	Ca <sup>2+</sup>	Mg <sup>2+</sup>	Na <sup>+</sup>	K <sup>+</sup>	SO <sub>4</sub> <sup>2-</sup>	Cl <sup>-</sup>	NO <sub>3</sub> <sup>-</sup>	HCO <sub>3</sub> <sup>-</sup>	Br <sup>-</sup>
C.E	1										
TDS	<b>0.99</b>	1									
Ca <sup>2+</sup>	<b>0.89</b>	<b>0.91</b>	1								
Mg <sup>2+</sup>	<b>0.98</b>	<b>0.96</b>	<b>0.85</b>	1							
Na <sup>+</sup>	<b>0.98</b>	<b>0.99</b>	<b>0.84</b>	<b>0.96</b>	1						
K <sup>+</sup>	<b>0.73</b>	<b>0.75</b>	<b>0.82</b>	<b>0.66</b>	<b>0.67</b>	1					
SO <sub>4</sub> <sup>2-</sup>	<b>0.87</b>	<b>0.91</b>	<b>0.96</b>	<b>0.81</b>	<b>0.84</b>	<b>0.88</b>	1				
Cl <sup>-</sup>	<b>0.98</b>	<b>0.97</b>	<b>0.82</b>	<b>0.98</b>	<b>0.99</b>	<b>0.63</b>	<b>0.79</b>	1			
NO <sub>3</sub> <sup>-</sup>	-0.08	-0.04	0.06	-0.09	-0.05	-0.18	-0.03	-0.07	1		
HCO <sub>3</sub> <sup>-</sup>	<b>0.51</b>	<b>0.53</b>	0.48	0.47	<b>0.53</b>	0.37	0.42	0.5	-0.05	1	
Br <sup>-</sup>	<b>0.78</b>	<b>0.78</b>	<b>0.79</b>	<b>0.78</b>	<b>0.70</b>	<b>0.82</b>	<b>0.78</b>	<b>0.75</b>	0.10	0.25	1

Bold indicates higher values

that all carbonate minerals (calcite, aragonite and dolomite) tend to reach saturation equilibrium (Table 2) which confirms the enrichment in Ca<sup>2+</sup> and Mg<sup>2+</sup> is mainly due to the exchange of cations and not to the dissolution of the carbonates (Montety et al. 2008; Sekiou and Kellil 2014). Conversely, the evaporitic minerals (halite, anhydrite and gypsum) are still in sub-saturation state and may increase the salinity of the groundwater confirming the water–rock interactions. From the geological map, the extent of the Triassic saliferous rocks in Jb. Ammar may confirm the increase in salinity particularly in the slopes parts following the flow direction.

### Spatial analysis with GIS

The GIS software (ArcGIS 10.1) allows the generation of the spatial distribution maps of piezometry, salinity, chlorides, sodium, nitrates and sulfates. The interpolation of the point data was established via linear kriging method.

A piezometric campaign was carried out during the months of September and October 2014 which led to the realization of a piezometric map (Fig. 5). The flow direction is essentially controlled by the topographic changes. The global flow is converging toward the sea which forms the downstream hydraulic level. Isopieze curves which height exceeds 40 m are located at Kechabta hills in the north, Jb. Ammar and Jb. Naheli in the south and > 25 m in Koudiat Touba. They do not reach 5 m locally in the Mabtouha plain in the upstream part of the watershed and toward the sea in the eastern part. In this area, the water table lies close to the surface and flush in several zones as a swamp or Garaa. The drainage, the irrigation and the sanitation are the most techniques used to compensate the excess, the deficit or the poor quality of water. The zero isopieze line is located along the shoreline and down to -3 m toward the depression of Ghar El Melh.

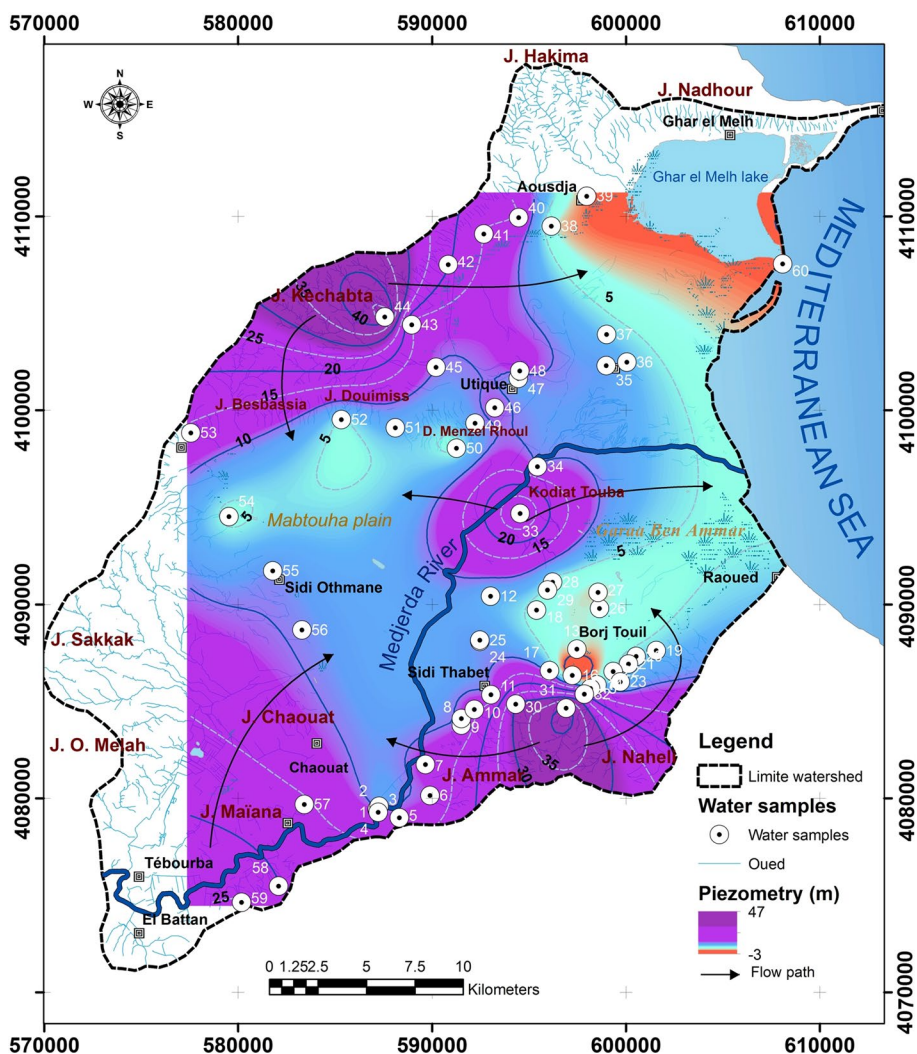
The piezometric depressions are usually associated with the most saline waters (TDS > 2 g/l). The salinity map (Fig. 6a) shows a clear increase according to the groundwater flow direction. Therefore, the groundwater samples were classified in three groups based mainly on the TDS contents.

- The first one, with the lowest TDS values (brackish) (< 2 g/l), occurs at the western part of the region. They are observed from the topographic highs (recharge area), suggesting the dilution effect of the groundwater;
- The second one with medium enrichment of salts (salty) (2 < TDS < 4 g/l). The groundwater samples are detected from the region situated between the above topography due to disparity in the enrichments of salts from the origins, following the water flow-path circumstances.
- The third one with high TDS > 4 g/l (saline) occurs in the eastern part of the catchment area from the topographic lows, close to the sea.

The TDS values are dramatically increased toward the coastline (exceeding 4000 mg/l) related to the groundwater mixing with seawater and/or to the solute diffusion from the marine clay aquitard, the marine aerosols, the excessive use of salts in agriculture and the paleosalinity near the shoreline. These processes are aggravated by the phenomenon of evaporation where the water table from the MLVA runs at low depths (within 1 m) below sea level. According to Samaali (2011), the spatial distribution map of the evapotranspiration (ETR) shows a progressive gradient in relation to the importance of soil humidity. Toward the plains, along the coastal areas (in the endorheic depressions), ETR increases strongly. The influence of the piezometric level can be felt by a high rate of ETR (1300 mm/year) in non-irrigated areas in the dry period (El Guarouani et al. 1999; Samaali 2011).



**Fig. 5** Piezometric map of the MLV shallow aquifer (September 2014) showing the flow directions from upstream to downstream areas



Maps of chlorides and sodium show strong similarities with TDS (Fig. 6b, c), with the same sectors of high salt load and the same gradual eastward toward the sea. It is always the coastal areas that show the high levels of chlorides and sodium. As with EC, the potential origin of these two ions in water may be related to the phenomenon of marine intrusion. According to Appelo and Postma (2005) and Ben Hamouda et al. (2015), the dominant ions in sea water are  $\text{Na}^+$  and  $\text{Cl}^-$ , and when intrusion occurs, the dominant ions in groundwater will be the  $\text{Na}^+$  and  $\text{Cl}^-$  ions. These data argue for the role of halite ( $\text{NaCl}$ ) dissolution as a major process contributing to groundwater mineralization in semiarid areas (Appelo and Postma 2005).

Nitrate contamination of groundwater has become of growing concern for people especially in rural areas. The study of this parameter has been widely applied in hydrogeological studies (e.g., Grava 2005; Zouhri et al. 2008; Kouzana et al. 2009; Farhat et al. 2010; Zghibi et al. 2012,

2013). The EU Directive 91/676/EEC, which protects waters against pollution caused by increase in nitrates from agricultural origins, fixes the acceptable threshold of nitrate concentration in groundwater at 50 mg/l (EU 1991; WHO 2004). In this study area, the concentrations of nitrates are widespread with greatly localized concentrations, frequently beyond the allowed threshold value of permissible limit for drinking water. About 67% of the samples have nitrate concentration above the threshold value of anthropogenic source (20 mg/l), and more than 50% of the samples have nitrate concentration exceeding the recommendations for drinking water.

According to the nitrate map (Fig. 6d), toward the hydrologic discharge zones, the increase in nitrates content is directly related to the intense agricultural practices typically found at the plain of Aousja, Kalaat Landalous and Mabtouha inducing excessive contributions of chemical fertilizers especially the nitrogen, an easily washable element.

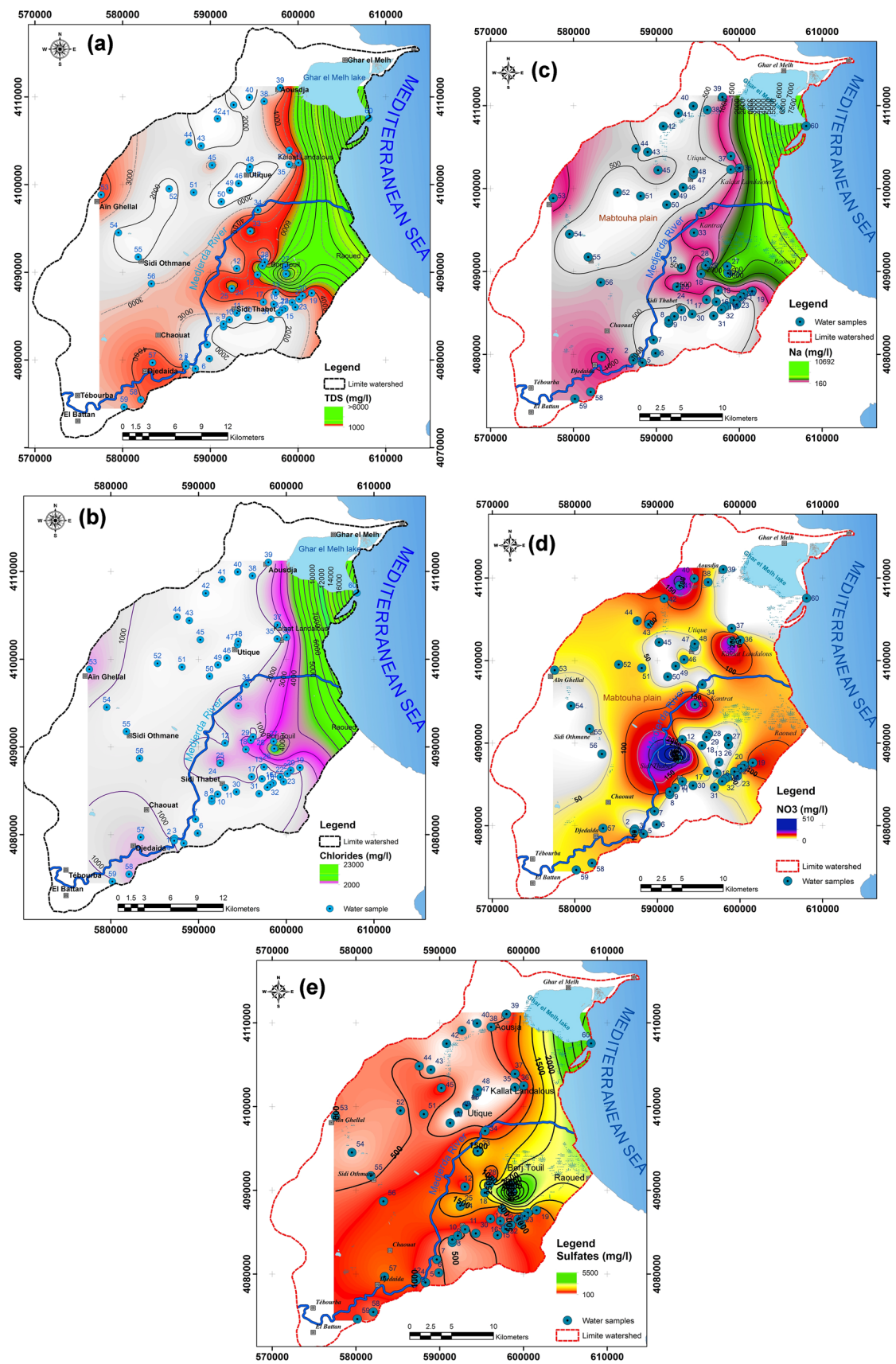


Fig. 6 Spatial distributions of a TDS, b chloride, c sodium, d nitrates and e sulfate of MLVA (September 2014)



Considering that these areas are dominated by the irrigated perimeters and an artificial drainage system, a stagnation of water in the river and a small thickness of the unsaturated zone, the water containing nitrates contaminates the groundwater. The source of nitrate pollution in this area may be caused by the drainage systems which lead to the drainage of the nitrogen fertilizers. High loading of nitrate concentration in Borj Touil and Sidi Thabet rural areas may be correlated with wastewater leakage from urbanization and high density of septic tanks. In these regions, water table is shallow and porous sandy soils allow rapid transport of N and other contaminants to groundwater. Therefore, septic systems become as one important source of Azote pollution. On the other hand, in the coastal zone (Raoued and Borj Touil areas) dominated by irrigation with treated wastewater, the nitrate concentrations are significantly higher. The wastewater treatment discharge, the animal operations and the crop fertilization may be the causes of high nitrate concentration. It is worth noting that the use of these waters for irrigation by submersion generated a large infiltration of these highly charged waters by the Nitrates.

From the sulfate map (Fig. 6e), the increase in salt content is accompanied by the increase in sulfate concentrations locally at the slopes sides of Jb. Ammar toward the shoreline. The highest  $\text{SO}_4^{2-}$  content in the groundwater samples in the areas where the piezometry is very low (less than 1 m) with a significant evaporation causes the dissolution of evaporites like the gypsum ( $\text{CaSO}_4 \cdot \text{H}_2\text{O}$ ) following the leaching of the evaporitic Triassic series from Jb. Ammar. Moreover, the highly positive loadings in  $\text{Mg}^{2+}$  and  $\text{SO}_4^{2-}$  ( $r^2 = 0.81$ ) and the excessive use of the  $\text{MgSO}_4$  fertilizers justify the significant role of the return flow from irrigation water.

### Inter-elemental plots

In order to highlight the different mechanisms contributing to groundwater mineralization, a series of ionic and ratio plots are presented (Fig. 7).

The plot of  $(\text{Ca}^{2+} + \text{Mg}^{2+})/(\text{HCO}_3^- + \text{SO}_4^{2-})$  versus  $(\text{Na}^+/\text{Cl}^-)$  (Fig. 7c) shows that the samples which have  $\text{Na}^+/\text{Cl}^-$  ratios higher than 1 indicate an enrichment of  $\text{Na}^+$ . This enrichment of the sodium relative to the halite dissolution is accompanied by a deficit in  $(\text{Ca}^{2+} + \text{Mg}^{+2})$  compared to  $\text{HCO}_3^-$  and  $\text{SO}_4^{2-}$ . The samples that have the ratios of  $\text{Na}^+/\text{Cl}^-$  lower than 1 are accompanied by an excess of  $(\text{Ca}^{2+} + \text{Mg}^{+2})$  relative to  $\text{HCO}_3^-$  and  $\text{SO}_4^{2-}$ . These results are due to the basic exchange phenomena related to the groundwater interactions with clay and silt in the alluvium or weathered materials (Fidelibus and Tulipano 1996, Stigter et al. 1998; Capaccioni et al. 2005).

The high positive correlation between  $\text{Ca}^{2+}$  and  $\text{SO}_4^{2-}$  (0.96) (Fig. 7a) is related to the dissolution of gypsum and/or anhydrite ( $\text{CaSO}_4 \cdot 2\text{H}_2\text{O}$ ) dispersed in the aquifer. The relative excess of  $\text{SO}_4^{2-}$  suggests that there are other sources of sulfates, in relation to both magnesium–sulfate salt dissolutions. This is shown by the high positive correlation between  $\text{Mg}^{2+}$  and  $\text{SO}_4^{2-}$  (0.81) (Fig. 7b) and the contribution of  $\text{MgSO}_4$  fertilizers (Adams et al. 2001; Gi-Tak et al. 2004). The existence of these fertilizers highlights the significant role of the return flow from irrigation water in the agricultural regions (EU 1991; Kouzana et al. 2009; Farhat et al. 2010; Abonoje Oyebo et al. 2012; Zghibi et al. 2014) especially in Borj Touil and Raoued where treated waste water irrigation is particularly used.

Bromide and chloride are usually used to distinguish between sources of natural and anthropogenic occurring contaminants in groundwater. Both are conservative elements in water and have different abundances in natural fluids and solids. Several studies (Davis et al. 1998; Alcalá and Custodio 2008; Katz et al. 2011) have described Cl/Br ratios for different processes that control salinity in groundwater. Alcalá and Custodio (2008) found that Cl/Br ratio, which is an important useful screening tool, and salinity in groundwater were affected by salt water intrusion, the proximity to urban and industrial areas (such as wastewater from septic tanks effluents), the dissolution of evaporitic rock outcroppings (Triassic saliferous), farm animal wastes, pesticides (fumigants), etc. The study of Alcalá and Custodio (2008) realized in Spain and Portugal on six salinity acquisition processes described in 24 selected aquifers can be used as a reference for the Mediterranean countries with average altitudes (such as Southern Europe and North Africa). In the MLVA, from the molar ratio  $\text{Br}^-/\text{Cl}^-$  (Fig. 7d), the distribution of the samples shows different possible origins of water salinity. In this case study, the contamination from the seawater is detected in the coastal samples. The waters having high concentrations of chlorides and high TDS values ( $\text{TDS} > 4000 \text{ mg/l}$  “G1”) are originated from the seawater intrusion and swamps. Following the distribution of the samples, the geographic distribution of all these samples is in the coastal zone confirming the first hypotheses. The second group “G2” forms a minority of samples with  $2000 < \text{TDS} < 4000 \text{ mg/l}$  having an origin of salinity corresponding to “urban wastewater” or “leaching of garbage and solid waste.” These samples are located in rural areas near the agglomerations. The last cluster is formed by the majority of the water samples, showing that the waters of the MLVA are mainly subject to the widespread agricultural pollution throughout the studied area.



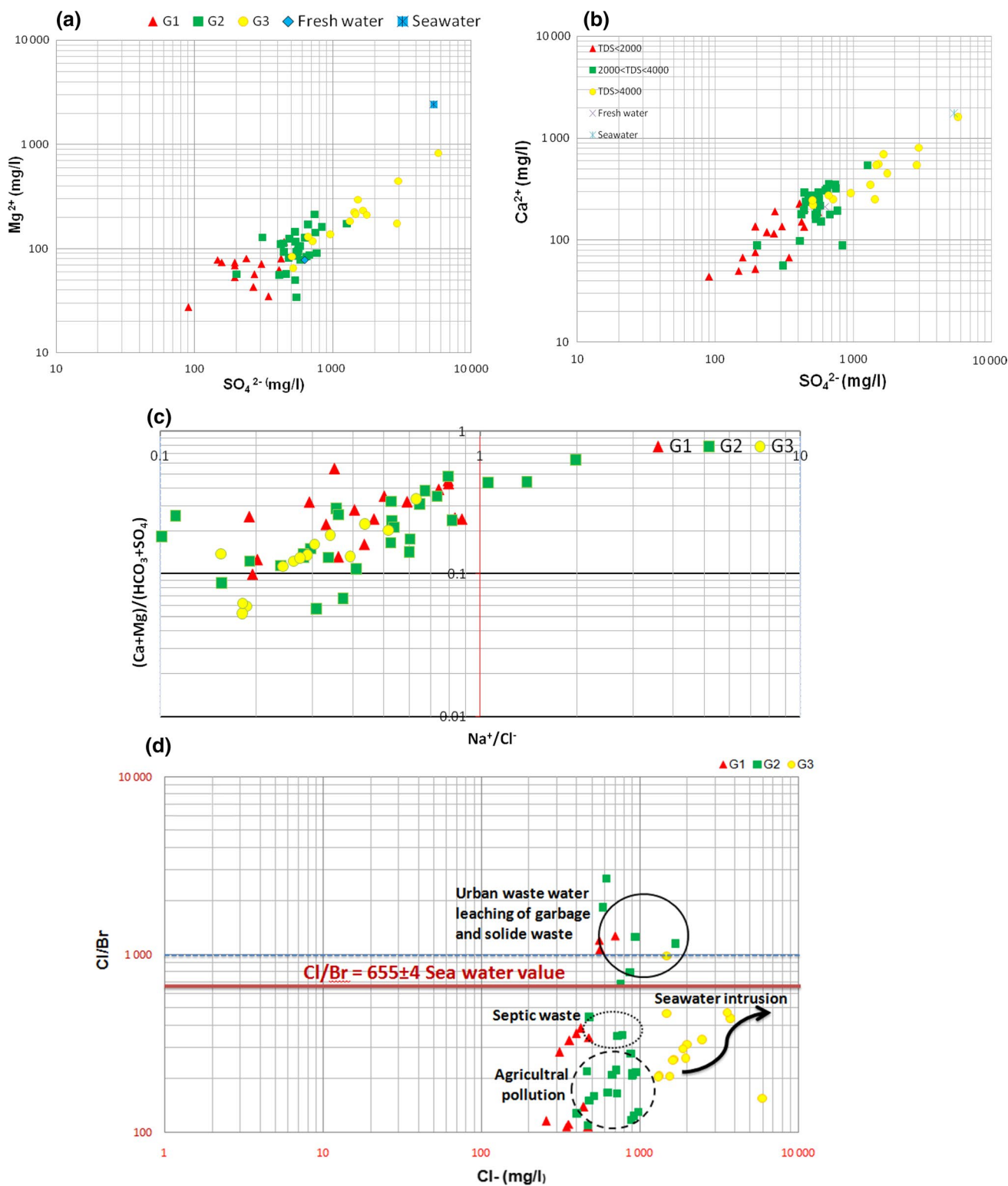


**Fig. 7** Plots of ionic relationships of the MLVA. **a**  $\text{Ca}^{2+}$  versus  $\text{SO}_4^{2-}$  relationship; **b**  $\text{Mg}^{2+}$  versus  $\text{SO}_4^{2-}$  relationship; **c**  $(\text{Ca} + \text{Mg}) / (\text{HCO}_3 + \text{SO}_4)$  versus  $(\text{Na} / \text{Cl})$  relationship; **d**  $\text{Cl}^- / \text{Br}^-$  versus  $\text{Cl}^-$

relationship of the MLVA represented in variation pattern of six salinity acquisition processes described in 24 aquifers selected in Spain and Portugal (Davis et al. 1998)

**Table 4** Eigenvalues of factors extracted through PCA, difference between factors, and proportion of variance explained by the factors

Factor	Eigen value	% total variance	Cumulative
1	7.414	<b>74.146</b>	74.14
2	1.034	<b>10.346</b>	84.49
3	0.747	7.47	91.96
4	0.609	6.091	98.05
5	0.11	1.102	99.15
6	0.062	0.623	99.78
7	0.014	0.142	99.92
8	0.006	0.065	99.98
9	0.0009	0.009	99.99
10	0.0001	0.001	100

Bold indicates higher values

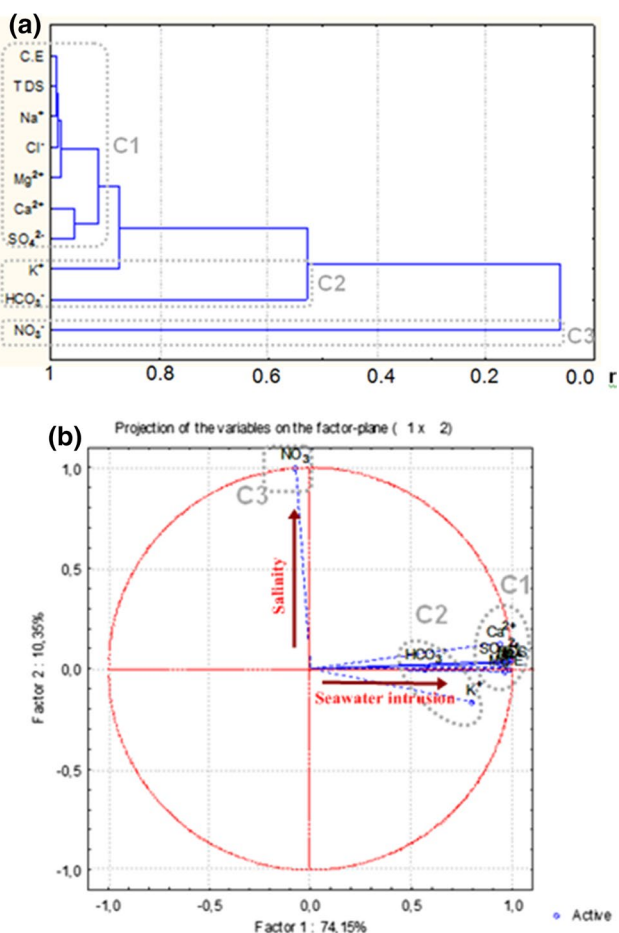


**Fig. 8** **a** Hierarchical clustering dendrogram of the major chemical components of the LVMA and **b** behavior of the variables with respect to the first two factors (F1 and F2)

### Multivariate analysis

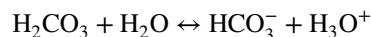
The variables (TDS, calcium, magnesium, sodium, potassium, sulfate, chloride, nitrate and bicarbonate) from 60

well sampling were analyzed adopting multivariate statistical techniques.

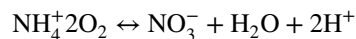
For a simpler and easier interpretation, the rotated factor pattern after factor extraction using varimax rotation is given in Table 4 and the % of the total variance vs eigenvalues from selected factor plots scores are plotted in Fig. 8. From the eigenvalues (> 1), it reveals that the first two factors account for approximately 84.5% of the total data variance. Clearly, the first factor represents a highly positive loadings with the variables (TDS,  $\text{Cl}^-$ ,  $\text{Na}^+$ ,  $\text{Ca}^{2+}$ ,  $\text{Mg}^{2+}$ ) than the second factor because these two factors are extracted successively, each one representing for as much of the remaining variance.

The projection of the variables on the factorial plane F1–F2 (Fig. 8) shows:

- Axis 1 accounts for 74.15% of the total variance in the dataset. It is determined by the  $\text{Cl}^-$ ,  $\text{Na}^+$ ,  $\text{SO}_4^{2-}$ ,  $\text{Mg}^{2+}$ ,  $\text{Ca}^{2+}$  related to evaporates ( $\text{NaCl}$  and  $\text{CaSO}_4$ ) and moderate charge on  $\text{K}^+$  and  $\text{HCO}_3^-$ . The association of these parameters is related to the seawater intrusion and can be termed, “the seawater salinization factor.” The bicarbonate ( $\text{HCO}_3^-$ ) concentrations in the groundwater are probably associated with the infiltrating water that has incorporated the dissolved  $\text{CO}_2$  from root respiration and the decay of soil organic matter. This is a constituent resulting from the dissolution of  $\text{CO}_2$  in the water and posterior dissociation of the formed  $\text{H}_2\text{CO}_3$  (Ruiz et al. 1990; Zghibi et al. 2014).



- Axis 2 accounts for 10.35% of the total variance in the dataset. It is determined by high loadings of  $\text{NO}_3^-$  suggesting a mixed groundwater with an anthropogenic source (such as chemical fertilizers). Under oxic conditions, the main component of fertilizers,  $\text{NH}_4^+$ , is easily oxidized to  $\text{NO}_3^-$  by the nitrification process according to (Kim et al. 2003; Zghibi et al. 2014).



This classification is confirmed by the HCA (Hierarchical cluster analysis) which is the mostly data classification technique applied in Earth sciences. The main result of the HCA performed on the 60 groundwater samples is the dendrogram (Fig. 8). Dendrogram of cluster analysis between variables with correlation matrix (Table 4) highlights that variables gather into the same three clusters confirming the last classification.

From PCA and HCA, it is interesting to investigate the relationship between nitrate concentration and seawater intrusion, the main two factors increasing the salinity of groundwater in the MLVA. On the first hand, samples distribution reveals that groundwater near the coast is mixed

with seawater and less concentrated with regard to nitrate. On the other hand, it clearly indicates that groundwater in Mabtouha plain and in the slopes sides with fast-growing agriculture with excessive use of chemical fertilizers was severely polluted in terms of  $\text{NO}_3^-$ . Thence, assessing the quality of the groundwater becomes important to ensure the safe use of this vital resource.

## Conclusion

This study is an integrate investigation of the MLVA adopting several methods such as satellite data (SRTM data, 30-m resolution), conventional maps, hydrogeochemical data, GIS tools and multivariate statistical techniques, to determine the anthropogenic inputs and the natural sources causing the groundwater contamination.

In the MLVA, the groundwater shows significant variations in the mineralization mainly attributed to the complexity of the hydrogeologic system where we enregistre very wide ranges of most hydrochemical parameters. The total dissolved solids (TDS) are mainly controlled by chlorides and sodium which are increased toward the sea confirming the seawater intrusion. The inter-elemental approach of major and minor elements and the calculation of the saturation indices allow to better comprehend the chemistry of these waters and to present the first hypotheses that can then be enhanced, particularly across the statistical approach.

The integration of two multivariate statistical methods (HCA and PCA) with the geochemical, hydrogeological and geological data allows the division of the region into three main geochemical areas, providing an improved regional image of the hydrogeochemical evolution of groundwater. The mineralization increases from the mountainous area to the coast following the global flow direction. Near the coast, high salinity levels ( $\text{TDS} > 4 \text{ g/l}$ ) are mainly related to seawater intrusion and swamps. In the plain, with moderate values of salinity ( $2 < \text{TDS} < 4 \text{ g/l}$ ), groundwater is controlled by the nature of the geological formations of the region such as gypsum (Triassic saliferous in J. Ammar) confirming water–rock interactions. Hydrolysis of such rocks explains the dominance of  $\text{Na}^+$  as cation and  $\text{Cl}^-$  and  $\text{SO}_4^{2-}$  as anions in groundwater. These ions are derived from the weathering of rocks and hydrolysis of evaporite minerals primarily in the continental part of the aquifer. High positive correlation between  $\text{Mg}^{2+}$  and  $\text{SO}_4^{2-}$  (0.81) proves the contribution of  $\text{MgSO}_4^-$  fertilizers. The returns of irrigation water, treated wastewater and wastewater leakage from urbanization are also causing a damage of the groundwater. In rural areas, the elevated nitrate concentration increasing groundwater salinity may be confirmed by the discharge of domestic

wastewater from septic tank effluents and the excessive use of chemical fertilizers.

These sources are aggravated by the phenomenon of evaporation mainly in sectors close to the sea where the water table runs at low depths (within 1 m) close to the land surface.

The lowest values of salinity ( $\text{TDS} < 2 \text{ g/l}$ ) occur at the west of the region in the hills of the upstream part of the watershed (recharge area) suggesting the dilution effect of the groundwater. All these findings make coastal areas vulnerable to intrusion which is accentuated by the droughts in the MLV region.

Investigation based on isotopic data ( $\delta^{14}\text{C}$ ,  $\delta \text{D}$ ,  $\delta^{18}\text{O}$ , etc.) are needed to confirm the extent of seawater intrusion along the coastal area.

Finally, it is highly recommended to control the anthropogenic activities frequently in order to minimize the pollution problems. Otherwise, this research work can provide an important information to improve water management strategies, to ensure sustainable water management and safe use.

**Acknowledgements** The authors are very grateful to the Director of National Nuclear Research Institute for making funds available for this work. We also thank all the Technicians of the Isotope Hydrology and Geochemistry Unit, Technopark Sidi Thabet, Tunisia, for helping us during the sampling campaigns as well as the analysis.

## References

- Abonoje Oyebo G S, Ako Ako A, Elambo Nkeng G, Cheo Suh E (2012) Hydrogeochemical characteristics of some Cameroon bottled waters, investigated by multivariate statistical analyses. *J Geochem Explor* 112:118–130. <https://doi.org/10.1016/j.gexplo.2011.08.003>
- Adams S, Tredoux G, Harris C, Titus R, Pietersen K (2001) Hydrochemical characteristics of aquifers near Sutherland in the Western Karoo, South Africa. *J Hydrol* 241:91–103. [https://doi.org/10.1016/S0022-1694\(00\)00370-X](https://doi.org/10.1016/S0022-1694(00)00370-X)
- Alcala FJ, Custodio E (2008) Using the Cl/Br ratio as a tracer to identify the origin of salinity in aquifers in Spain and Portugal. *J Hydrol* 359:189–207. <https://doi.org/10.1016/j.jhydrol.2008.06.028>
- Ammar B (1989) Etude de l'environnement de Tunis et de sa région en relation avec l'art de l'ingénieur en génie civil. Ph.D. dissertation, University of Science and Technology, Languedoc
- Andolsi M (2016) Caractérisations physico-chimiques des eaux thermales du Nord de la Tunisie et des boues préparées par interaction eaux thermales-argiles et leurs applications. Ph.D. dissertation, University of Tunis El Manar, Tunisia
- Appelo CAJ, Postma D (2005) Geochemistry, groundwater and pollution, 2nd edn. Balkema, Rotterdam
- Bahri A (1993) Évolution de la salinité dans un périmètre irrigué de la Basse Vallée de la Medjerda en Tunisie. *Sci du sol* 31(3):125–140
- Ben Ammar S, Taupin JD, Zouari K, Khouatmia M, Ben Assi M (2014) Etude géochimique et isotopique d'un aquifère phréatique côtier anthropisé: Nappe de Oussja-Ghar El Melah (Tunisie).





- In: Proceedings of FRIEND-Water 2014, hydrology in a changing world: environmental and human dimensions, Montpellier, France, October 2014 (IAHS Publ. 363, 269–275, 2014)
- Ben Ammar S, Taupin JD, Zouari K, Khoutmia M (2016) Identifying recharge and salinization sources of groundwater in the Oussja Ghar el Melah plain (northeast Tunisia) using geochemical tools and environmental isotopes. *Environ Earth Sci*. <https://doi.org/10.1007/s12665-016-5431-x>
- Ben Hamouda MF, Kondash AJ, Lauer N, Mejri L, Tarhouni J, Vengosh A (2015) Assessment of groundwater salinity mechanisms in the coastal aquifer of El Haouaria, Northern Tunisia. In: 11th applied isotope geochemistry conference, AIG-11 BRGM. *Proceedia earth and planetary science*, vol 13, pp 194–198. <https://doi.org/10.1016/j.proeps.2015.07.046>
- Bodrud-Dozaa Md, Towfiqul Islam ARM, Ahmed Fahad, Das Samiran, Sahae Narottam, Safiur Rahman M (2016) Characterization of groundwater quality using water evaluation indices, multivariate statistics and geostatistics in central Bangladesh. *Water Sci* 30:19–40. <https://doi.org/10.1016/j.wsj.2016.05.001>
- Bouchaou L, Michelot JL, Vengosh A, Hsissou Y, Qurtobi M, Gaye CB, Bullen TD, Zuppi GM (2008) Application of multiple isotopic and geochemical tracers for investigation of recharge, salinization, and residence time of water in the Souss–Massa aquifer, southwest of Morocco. *J Hydrol* 352:267–287. <https://doi.org/10.1016/j.jhydrol.2008.01.022>
- Boutib L (1998) Tectonique de la région du Grand Tunis: évolution géométrique et cinématique des blocs structuraux du Mésozoïque à l'actuel (Atlas nord oriental de la Tunisie). Ph.D. dissertation, Université Tunis
- Bureau de Recherche Géologique et Minière (BRGM) (2001) Contribution à la caractérisation des états de références géochimiques des eaux souterraines. Rapport d'avancement no1 Etude bibliographique, Etude réalisée dans le cadre des opérations de service public du BRGM 00EAU714, BRGM/RP-50403-FR
- Capaccioni B, Didero M, Paletta C, Idero L (2005) Saline intrusion and refreshing in a multilayer coastal aquifer in the catania Plain (Sicily, Southern Italy): dynamics of degradation processes according to hydrochemical characteristics of groundwaters. *J Hydrol* 307:1–16. <https://doi.org/10.1016/j.jhydrol.2004.08.037>
- Charfi S, Zouari K, Feki S, Mami E (2013) Study of variation in groundwater quality in a coastal aquifer in north-eastern Tunisia using multivariate factor analysis. *Quatern Int* 302:199–209. <https://doi.org/10.1016/j.quaint.2012.11.002>
- Chenini I, Zghibi A, Kouzana L (2015) Hydrogeological investigations and groundwater vulnerability assessment and mapping for groundwater resource protection and management: state of the art and a case study. *J Afr Earth Sci* 109:11–26. <https://doi.org/10.1016/j.jafrearsci.2015.05.008>
- Davis JC (1986) *Statistics and data analysis in geology*. Wiley, New York, p 621p
- Davis SN, Whittemore DO, Fabryka-Martin J (1998) Uses of chloride/bromide ratios in studies of potable water. *Ground Water* 36:338–350
- De Montety V, Radakovitch O, Vallet-Coulomb C, Blavoux B, Hermitte D, Valles V (2008) Origin of groundwater salinity and hydrogeochemical processes in a confined coastal aquifer: case of the Rhône delta (Southern France). *Appl Geochem J*. <https://doi.org/10.1016/j.apgeochem.2008.03.011>
- El Guarouani A, Jabrane R, Bousemma, Merzouk A (1999) Contribution de l'imagerie satellitaire à la détection des zones saturées et au zonage de l'Evapotranspiration dans la basse vallée de la Medjerda (Tunisie). *Sécheresse* no 2 10(2):117–122
- E.U. (1991) Council directive 1991/676/EEC, of 12 December 1991, concerning the protection of waters against pollution caused by nitrates from agricultural sources. *Off J Eur Union* 375:1–8
- Fakir Y, Zerouali A, Aboufirassi M, Bouabdelli M (2001) Exploitation et salinité des aquifères de la Chaouia côtière, littoral atlantique, Maroc. *J Afr Earth Sci* 32(4):791–801. [https://doi.org/10.1016/S0899-5362\(02\)00055-6](https://doi.org/10.1016/S0899-5362(02)00055-6)
- Farhat B, Ben Mammou A, Kouzana L, Chenini I, Podda F, De Giudici G (2010) Groundwater chemistry of the Mornag aquifer system in NE Tunisia. *Resour Geol* 4:377–388. <https://doi.org/10.1111/1/j.1751-3928.2010.00142.x4>
- Fidelibus MD, Tulipano L (1996) Regional flow of intruding sea water in the carbonate aquifers of Apulia (Southern Italy). In: Proceedings of the 14th salt water intrusion meeting, vol 87, pp 230–241
- Freeze RA, Cherry JA (1979) *Groundwater*. Prentice Hall, Englewood Cliffs
- Gi-Tak C, Kangjoo K, Seong T, Kyoung H, Soon O, Byoung Y, Hyoung S, Chul W (2004) Hydrogeochemistry of alluvial groundwaters in an agricultural area: an implication for groundwater contamination susceptibility. *Chemosphere* 55:369–378. <https://doi.org/10.1016/j.chemosphere.2003.11.001>
- Grava ME (2005) Hydrochemical, hydrogeological and geostatistical analysis of Eastern Cape Bon Aquifer (Northern Tunisia). Diplôme postgrade d'hydrogéologue, Formation spécialisée en hydrogéologie. Centre d'Hydrogéologie de l'Université de Neuchâtel, Suisse
- Holly A, Michael Ann-Mulligan E, Charles-Harvey F (2005) Seasonal oscillations in water exchange between aquifers and the coastal ocean. *Nature* 436:1145–1148. <https://doi.org/10.1038/nature03935>
- Institut National de Météorologie (INM) (2015) Données climatiques sur le Nord Est de la Tunisie. Rapport interne. <http://www.meteo.tn/default.html>
- Jia H, Liang S, Zhang Y (2015) Assessing the impact on groundwater safety of inter-basin water transfer using a coupled modeling approach. *Front Environ Sci Eng* 9(1):84–95. <https://doi.org/10.1007/s11783-014-0741-2>
- Kacem J (2004) Etude sismotectonique et évaluation de l'aléa sismique régional du Nord-Est de Tunis : Apport de la sismique réflexion dans l'identification des sources sismogéniques. Thèse de Doctorat, Université Tunis el Manar
- Kaliraj S, Chandrasekar N, Magesh NS (2014) Identification of potential groundwater recharge zones in Vaigai upper basin, Tamil Nadu, using GIS-based analytical hierarchical process (AHP) technique. *Arab J Geosci*. <https://doi.org/10.1007/s12517-013-0849-x>
- Katz BG, Eberts SM, Kauffman LJ (2011) Using Cl/Br ratios and other indicators to assess potential impacts on groundwater quality from septic systems: a review and examples from principal aquifers in the United States. *J Hydrol* 397:151–166. <https://doi.org/10.1016/j.jhydrol.2010.11.017>
- Kim Y, Lee KS, Koh DC, Lee DH, Lee SG, Park WB, Koh GW, Woo NC (2003) Hydrogeochemical and isotopic evidence of groundwater salinization in a coastal aquifer: a case study in Jeju volcanic



- island, Korea. *J Hydrol* 270:282–294. [https://doi.org/10.1016/S0022-1694\(02\)00307-4](https://doi.org/10.1016/S0022-1694(02)00307-4)
- Kouzana L, Ben Mammou A, Sfar-Felfoul M (2009) Seawater intrusion and associated processes: case of the Korba aquifer (Cap-Bon, Tunisia). *CR Geosci* 341:21–35. <https://doi.org/10.1016/j.crte.2008.09.008>
- Lee JY, Song SH (2007) Evaluation of groundwater quality in coastal areas: implications for sustainable agriculture. *Environ Geol* 52:1231–1242. <https://doi.org/10.1007/s00254-006-0560-2>
- Loucks DP, Jia H (2012) Managing water for life. *Front Environ Sci Eng* 6(2):255–264. <https://doi.org/10.1007/s11783-011-0359-6>
- Machiwal D, Jha MK (2015) Identifying sources of groundwater contamination in a hard-rock aquifer system using multivariate statistical analyses and GIS-based geostatistical modeling techniques. *J Hydrol Reg Stud* 4:80–110. <https://doi.org/10.1016/j.ejrh.2014.11.005>
- Masoud AA (2014) Groundwater quality assessment of the shallow aquifers west of the Nile Delta (Egypt) using multivariate statistical and geostatistical techniques. *J Afr Earth Sci* 95:123–137. <https://doi.org/10.1016/j.jafrearsci.2014.03.006>
- Mejri L (2012) Tectonique Quaternaire, paléoseismicité et sources sismogéniques en Tunisie Nord-Orientale: Etude de la faille d'Utique. Thèse de Doctorat. Université de Toulouse 3 Paul Sabattier
- Melki F (1997) Tectonique de l'extrémité nord-est de la Tunisie (Bizerte-Menzel Bourguiba-Mateur). Evolution tectonique de blocs structuraux du Crétacé supérieur au Quaternaire. Thèse de Doctorat, Université Tunis II
- Molla MA, Saha N, Salam SA, Rakib-uz-Zaman M (2015) Surface and groundwater quality assessment based on multivariate statistical techniques in the vicinity of Mohanpur, Bangladesh. *Int J Environ Health Eng* 4:18. <https://doi.org/10.4103/2277-9183.157717>
- Montety VD, Radakovitch O, Vallet-Coulomb C, Blavoux B, Hermitte D, Valles V (2008) Origin of groundwater salinity and hydrogeochemical processes in a confined coastal aquifer, Case of the Rhône delta (Southern France). *Appl Geochem* 23:2337–2349. <https://doi.org/10.1016/j.apgeochem.2008.03.011>
- Morell I, Gimhez E, Esteller MV (1996) Application of principal components analysis to the study of salinization on the Castellon Plain (Spain). *Sci Total Environ*, 177, 161–171. *SSDI* 0048-9697 (95) 04893-6
- Ouerghi S (2014) Intégration des données multisources (Géologiques, sismologiques, géophysiques et géomorphométriques) dans un environnement SIG pour l'analyse structurale du Nord Est de la Tunisie. Thèse de Doctorat, Université de Sfax, Ecole Nationale d'Ingénieurs de Sfax
- Papatheodorou G, Lambrakis N, Panagopoulos G (2007) Application of multivariate statistical procedures to the hydrochemical study of a coastal aquifer: an example from Crete, Greece. *Hydrol Process* 21:1482–1495. <https://doi.org/10.1002/hyp.6322>
- Park SC, Yun ST, Chae GT, Yoo IS, Shin KS, Heo CH, Lee SK (2005) Regional hydrochemical study on salinization of coastal aquifers, western coastal area of South Korea. *J Hydrol* 313(3–4):182–194. <https://doi.org/10.1016/j.jhydrol.2005.03.001>
- Pini S, Kchouk F, Jauzein A (1971) Carte géologique au 1/50000 et notice explicative de l'Ariana. Notes du service Géologique de Tunisie
- Pulido-Leboeuf P (2004) Seawater intrusion and associated processes in a small coastal complex aquifer (Castell de Ferro, Spain). *Appl Geochem* 19:1517–1527. <https://doi.org/10.1016/j.apgeochem.2004.02.004>
- Richter BC, Kreitler CW (1991) Identification of Sources of Ground-Water Salinization using Geochemical Techniques. U.S. Environmental Protection, Washington, D.C. <https://doi.org/10.2113/11.2.107>
- Ruiz F, Gomis V, Blasco P (1990) Application of factor analysis to the hydrogeochemical study of a coastal aquifer. *J Hydrol* 119:169–177. [https://doi.org/10.1016/0022-1694\(90\)90041-U](https://doi.org/10.1016/0022-1694(90)90041-U)
- Samaali H (2011) Etude de l'évolution de l'occupation et de l'utilisation du sol dans le delta de Medjerda par télédétection et systèmes d'Information Géographiques. Doct. Es-Sciences, Université de Tunis, Faculté des Sciences Humaines et Sociales, Tunisie
- Samsudin AR, Haryono A, Hamzah U, Rafek AG (2008) Salinity mapping of coastal groundwater aquifers using hydrogeochemical and geophysical methods: a case study from north Kelantan, Malaysia. *Environ Geol J*. <https://doi.org/10.1007/s00254-007-1124-9>
- Sekiou F, Kellil A (2014) Caractérisation et classification empirique, graphique et statistique mutivariable d'eaux de source embouteillées de l'Algérie, Larhyss J. 225–246. <http://dspac.e.univ-biskra.dz:8080/jspui/handle/123456789/4204>
- Selvam S, Manimaran G, Sivasubramanian P, Balasubramanian N, Seshunarayana T (2014) GIS-based Evaluation of Water Quality Index of groundwater resources around Tuticorin coastal city, south India. *Environ Earth Sci*. <https://doi.org/10.1007/s12665-013-2662-y>
- Stigter TY, Van-Ooijen SPI, Popst VEA, Appelo CAJ, Carvalho AMMD (1998) A hydrogeological and hydrochemical explanation of the groundwater composition under irrigated land in a Mediterranean environment, Algarve, Portugal. *J Hydrol* 208:262–279. [https://doi.org/10.1016/S0022-1694\(98\)00168-1](https://doi.org/10.1016/S0022-1694(98)00168-1)
- Tringali C, Re V, Siciliano G et al (2017) Insights and participatory actions driven by a socio-hydrogeological approach for groundwater management: the Grombalia Basin case study (Tunisia). *Hydrogeol J*. <https://doi.org/10.1007/s10040-017-1542-z>
- USSL (United States Salinity Laboratory Staff) (1954) Diagnosis and improvement of saline and alkali soils, hand book 60. US Department of Agricultural Soils, US Department of Agricultural (USDA), Washington, pp 69–81
- World Health Organization (WHO) (2004) Guidelines for drinking water quality, vol 1, recommendations. WHO, Geneva, pp 145–220
- Zghibi A, Zouhri L, Tarhouni J, Kouzana L (2012) Groundwater mineralization processes in Mediterranean semiarid systems (Cap-Bon, North east of Tunisia): hydrogeological and geochemical approaches. *Hydrol Proces*. <https://doi.org/10.1002/hyp.9456>
- Zghibi A, Tarhouni J, Zouhri L (2013) Assessment of seawater intrusion and nitrate contamination on the groundwater quality in the Korba coastal plain of Cap-Bon (North-east of Tunisia). *J Afr Earth Sci* 87:1–12. <https://doi.org/10.1016/j.jafrearsci.2013.07.009>



- Zghibi A, Merzougui A, Zouhri L, Tarhouni J (2014) Understanding groundwater chemistry using multivariate statistics techniques to the study of contamination in the Korba unconfined aquifer system of Cap-Bon (North-east of Tunisia). *J Afr Earth Sci* 89:1–15. <https://doi.org/10.1016/j.jafrearsci.2013.09.004>
- Zouhri L, Carlier E, Ben Kabbour B, Toto EA, Gorini C, Louche B (2008) Groundwater interaction in the coastal environment: hydrochemical, electrical and seismic approaches. *Bull Eng Geol Environ* 67:123–128. <https://doi.org/10.1007/s10064-007-0101-6>

